Processing and Application of Ceramics 7 [4] (2013) 147–151
DOI: 10.2298/PAC1304147N

Preparation of glass-ceramic in Li_2O-Al_2O_3-GeO_2-P_2O_5 system

Jelena D. Nikolić[1,*], Sonja V. Smiljanjić[2], Srđan D. Matijašević[1], Vladimir D. Živanović[1], Mihajlo B. Tošič[1], Snežana R. Grujić[2], Jovica N. Stojanović[1]

[1]*Institute for the Technology of Nuclear and other Mineral Raw Materials, 86 Franchet d' Esperey St, 11000 Belgrade, Serbia*

[2]*Faculty of Technology and Metallurgy, University of Belgrade, Karnegijeva 4, 11000 Belgrade, Serbia*

Received 6 September 2013; received in revised form 22 November 2013; accepted 30 November 2013

Abstract

The results of preparation and structural characterization of glass-ceramics from the system Li_2O-Al_2O_3-GeO_2-P_2O_5 are shown in this paper. The crystallization behaviour of the selected glass was examined under non-isothermal and isothermal crystallization conditions. DTA, XRD and SEM methods were employed for analyses. It was confirmed that this glass crystallizes by the volume crystallization mechanism. The results also showed that the glass crystallize by primary crystallization. As a primary phase the $LiGe_2(PO_4)_3$ is formed and the traces of GeO_2 as a secondary one is present. The crystallization process occurred at a high homogeneous nucleation rate and the spherical morphology of crystal growth. By applying the Kissinger relation the activation energy of crystal growth E_a = 462 kJ/mol was determined.

Keywords*: germanium phosphate glass, crystallization, kinetics, crystal growth*

I. Introduction

High lithium ionic conducting solids are potential electrolyte materials for high energy density batteries and other electrochemical devices [1]. Based on conducting properties, one of the most promising materials for such purpose is the glass-ceramic prepared from Li_2O-Al_2O_3-GeO_2-P_2O_5 glassy system. These materials can be usually obtained by the classical powder sintering route, sol-gel method and common glass-ceramic processes [2]. Due to several technological advantages the glass-ceramics process was frequently used for fabrication of lithium ionic conducting materials [3,4]. The studies of crystallization of Li_2O-Al_2O_3-GeO_2-P_2O_5 glasses showed that one of dominant crystal phase precipitated in glass matrix is NASICON-type $LiGe_2(PO_4)_3$ crystals. Also, it was found that in this composition, the partial substitution of tetravalent germanium ions by trivalent aluminium allows more Li^+ into the crystal structured that causes an increase in ionic conductivity of the prepared glass-ceramics [5,6]. Therefore, to fabricate appropriate lithium ion conducting glass-ceramics, it is necessary to study in detail the crystallization behaviour of lithium germanium phosphate glasses of different composition. In this paper the glass with composition $22.5Li_2O{\cdot}10Al_2O_3{\cdot}30GeO_2{\cdot}37.5P_2O_5$ (mol%) prepared by standard melt-quenching technique was investigated.

II. Experimental procedure

Li_2O-Al_2O_3-GeO_2-P_2O_5 glass was prepared by the standard melt-quenching technique. Reagent grade Li_2CO_3, Al_2O_3, GeO_2 and $(NH_4)_2HPO_4$ were mixed and homogenized in agate mortar and the mixture was melted in covered Pt-crucible in an electrical furnace, Carbolite BLF 17/3 at T = 1400 °C for t = 1 h. The melt was cast and cooled between two steel plates. The solidified glass sample was transparent, light yellowish in colour and without residual bubbles. The chemical analysis was determined using spectrophotometer AAS PERKIN ELMER Analyst 300.

Crystallization behaviour under non-isothermal crystallization conditions was investigated and for this one part of bulk glass sample was crushed in agate mortar and then sieved to appropriate particle sizes. To determine crystallization mechanism the DTA experiments were

* Corresponding author: tel: +381 11 3691 722
fax: +381 11 3691 583, e-mail: *j.nikolic@itnms.ac.rs*

used and the following glass granulations were chosen: < 0.048, 0.048–0.063, 0.063–0.1, 0.1–0.2, 0.2–0.3, 0.3–0.4, 0.4–0.5, 0.5–0.65, 0.65–0.83 and 0.83–1 mm. The measurements were performed on a Netsch STA 409EP device by heating a constant sample mass of 100 mg at a rate of β = 10 °C/min in the temperature range T = 20–800 °C. The glass granulation < 0.048 mm was used for determination of kinetic parameters of crystallization and the DTA crystallization peaks were recorded at several heating rates 5, 10, 12, 15 and 20 °C/min.

To determine the temperature range of nucleation and the temperature of maximum nucleation rate the samples with the granulation 0.50–0.65 mm (100 mg) were heated in DTA apparatus at heating rate β = 10 °C/min. Before DTA run these samples were thermally treated at selected temperatures of nucleation T = 500–620 °C for different times t_n = 15, 30, 60, 120, 180 and 300 minutes.

The experiments under isothermal condition were performed in one-stage regime with bulk glass samples which were heated at heating rate β = 10 °C/min up to the chosen temperature in the range 500–800 °C and then held at these temperatures for different times from 15 min to 100 h. The XRD method was used to determine the phase composition of the crystallized glass. The XRD patterns were obtained on a Philips PW-1710 automated diffractometer using a Cu tube operated at 40 kV and 30 mA. The instrument was equipped with a diffracted beam curved graphite monochromator and a Xe-filled proportional counter. The diffraction data were collected in the 2θ Bragg angle range from 5 to 70°, counting for 1 s (qualitative identification) and from 10° to 110° for 4 s (quantitative phase analysis-Rietveld method) at every 0.02° step. The divergence and receiving slits were fixed 1 and 0.1, respectively. All the XRD measurements were performed at room temperature in a stationary sample holder. The quantitative amounts of crystalline phases in the glass sample were determined using the full structure matching mode of the Rietveld refinement technique [7], using the FULLPROF programme [8].

A MIRA 3 XMU microscope was used for the SEM investigations, and the fractured bulk samples previously sputtered with gold were used.

III. Results and discussion

The results of the chemical analyses of the glass are presented in Table 1. It can be seen that the glass composition is close to the nominal one.

X-ray powder diffraction (XRD) analysis confirmed the quenched melts to be amorphous. The XRD method was used to determine the phase composition of the crystallized glass (Fig. 1.) and the quantitative volume fractions of crystalline phases were obtained by the Rietveld analysis of XRD pattern for the fully crystallized glass sample annealed at T = 800 °C for t = 100 h (Table 2). The XRD results revealed the primary crystallization of this glass with precipitation of primary $LiGe_2(PO_4)_3$ crystalline phase (rhombohedral crystal system, space group $R3c$ (167) [9]. According to the JCPDS card, there is no aluminium in the structure of $LiGe_2(PO_4)_3$ although it is believed that aluminium can be present in solid solution within this structure. The formation of a solid solution can exist due to the similar ionic radii of Al^{3+} and Ge^{4+}. The partial substitution of Ge^{4+} by Al^{3+} induces more Li^+ into the crystal structure and, therefore, increased ionic conductivity of the resulting glass-ceramics. As shown in Table 2, the secondary GeO_2 phase [10] appeared in a small volume fraction (2.41 %) in the crystallized sample.

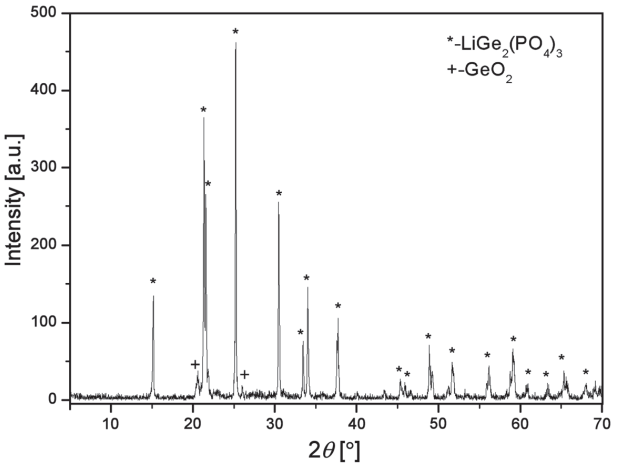

Figure 1. XRD pattern of the glass sample annealed at T = 800 °C for t = 100 h

It may be considered that the crystal structure of the main crystal phase $LiGe_2(PO_4)_3$ of this glass sample consists of GeO_6 octahedra and PO_4 tetrahedra (Fig. 2). Both units are linked by their corners to form a three-dimensional network structure and this structure results in cavities where lithium ions reside and in bottlenecks in which they pass through. Asymmetry of [PO_4] tetrahedron unit of phosphate glasses is believed to be the origin of their many specific properties. Three oxygen atoms are connected by single

Table 1. Chemical analysis of the glass

	Oxide content, x_i [mol %]			
	Li_2O	Al_2O_3	GeO_2	P_2O_5
Nominal	22.5	10	30	37.5
Analysed	21.98±1.0	9.37±0.5	32.54±0.5	36.11±0.5

Table 2. The most important crystallographic parameters for crystalline phases, obtained from Rietveld refinement of XRD pattern

Phase	Unit cell parameters			Quantitative volume fraction [%]
	a [Å]	*b* [Å]	*c* [Å]	
$LiGe_2(PO_4)_3$	8.2648(2)	8.2648(2)	20.5696(7)	97.59
GeO_2	5.003(2)	5.003(2)	5.580(5)	2.41

Table 3. The crystallization peak temperature T_{p1}, for different heating rates β of the powder samples having particle sizes < 0.048 mm

	β [°C/min]				
	5	10	12	15	20
T_{p1} [°C]	629	639	641	645	649

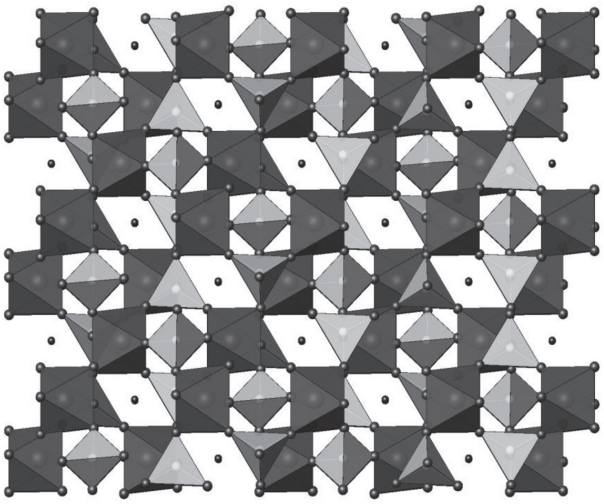

Figure 2. Structure of $LiGe_2(PO_4)_3$ along *b*-axes (dark grey GeO_6 octahedra, light grey PO_4 tetrahedra, black spheres Li^+ ions in cavities) [6]

bonds to the phosphor atom and via them the tetrahedron is connected to neighbouring tetrahedra. The fourth oxygen atom is connected by a double bond to phosphor atom [11].

To determine the dominant crystallization mechanism of this glass, DTA curves of the glass powder samples with particle sizes of 0–1 mm were recorded at a heating rate β = 10 °C/min in the temperature range 400–800 °C, Fig. 3. All DTA curves show two exothermal temperature peaks T_{p1} and T_{p2} representing the glass crystallization. The higher peaks T_{p1} appeared at lower temperatures while only the peaks height is changed while their positions do not change markedly by increasing of the glass particle size. Similar peaks behaviour was registered for all glass samples studied. Based on phase composition of crystallized glass sample determined by XRD it can be considered that $LiGe_2(PO_4)_3$ crystallized at peak T_{p1}, while the secondary phase GeO_2 is formed at T_{p2}.

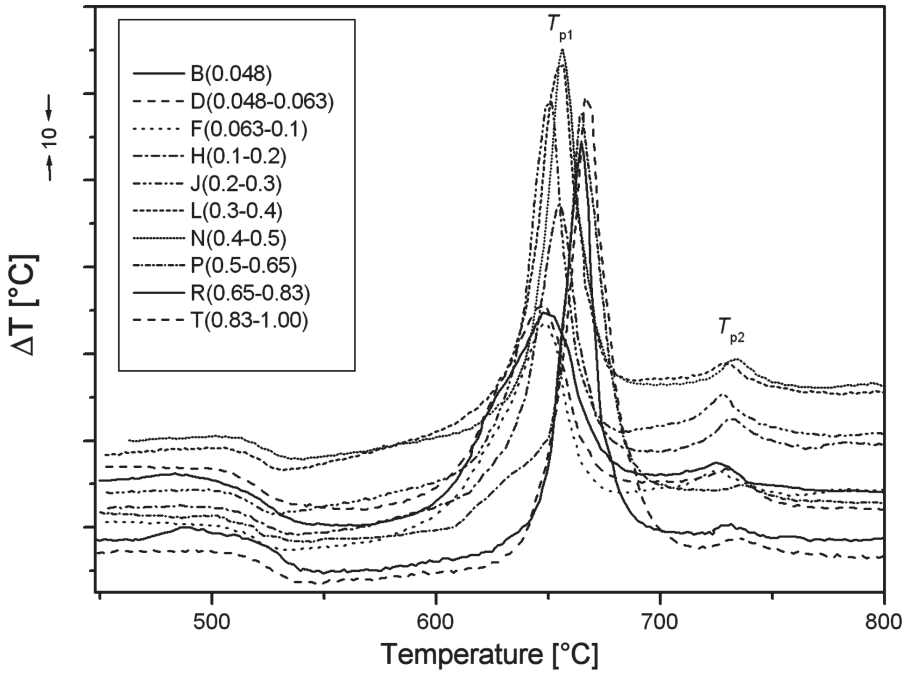

Figure 3. DTA curves recorded at a heating rate β = 10 °C/min for glass powder samples with different particle sizes

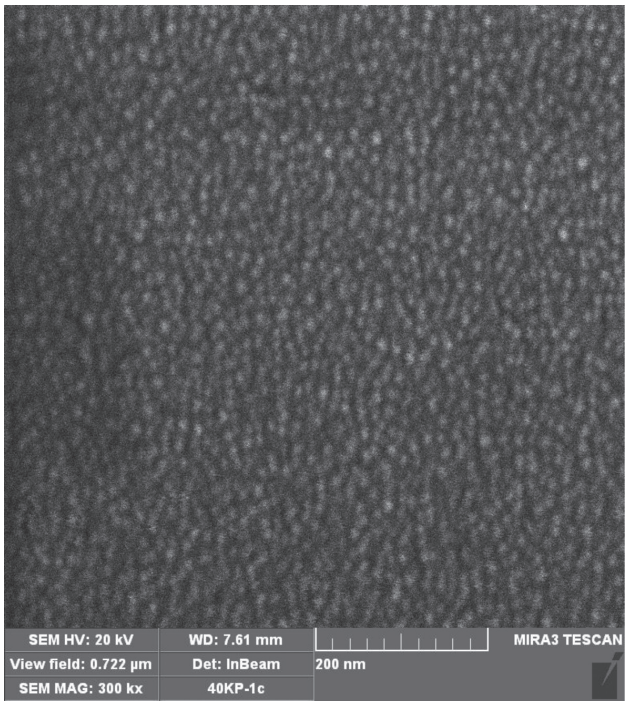

Figure 4. SEM micrograph of glass sample heat treated at T = 550 °C for t = 30 min

The characteristic temperatures of glass determined on DTA curve recorded for the glass sample with particle sizes < 0.048 mm are: the glass transition temperature T_g=514 °C, the crystallization peak temperatures T_{p1}=639 °C, T_{p2}=721 °C and liquidus temperature T_l=1041 °C.

The kinetic parameters of crystallization were determined by using the DTA data of the glass powder with particle sizes < 0.048 mm heated at heating rates β = 5, 10, 12, 15 and 20 °C/min. In Table 3 the crystallization peak temperatures T_{p1}, for different heating rates β are shown.

To study the microstructure of isothermally treated bulk samples in the temperature range of 500–800 °C for different times the SEM method was employed and the surface of crushed samples were recorded. In Fig. 4, SEM micrograph of glass sample heat treated at T = 550 °C for 30 minutes is shown. SEM micrographs revealed the presence of spherically shaped crystallites dimension of 30–50 nm in glass matrix. According to XRD analysis (Fig. 1) these crystals belong to $LiGe_2(PO)_4$. The crystal number density was increased with the increase of temperature and the duration of thermal treatment. The spherical growth morphology of these crystals indicated a screw dislocations controlled crystals growth proceeding on crystal/glass interface.

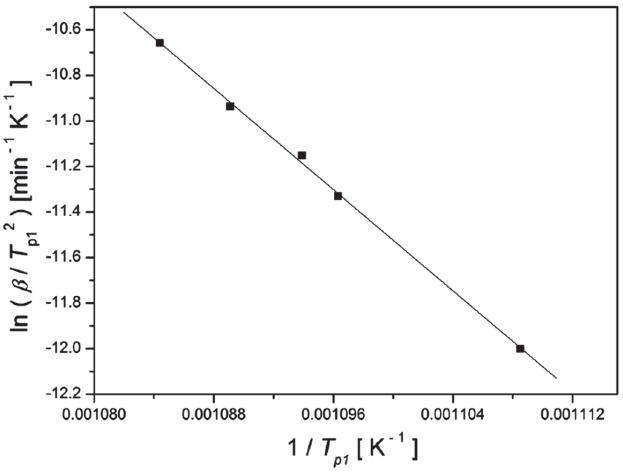

Figure 5. The Kissinger plot ln(β/T_p^2) *vs.* 1/T_p of glass sample with particle sizes <0.048 mm

IV. Discussion

Glasses generally crystallize by either surface or volume mechanism. The one of the procedure convenient for evaluating the dominant crystallization mechanism of glass powder is differential thermal analysis (DTA) [12]. The DTA parameters $T^2/(\Delta T)_p$ and the height of the exothermal peak $(\delta T)_p$ reflect dependency on glass particle size. Since the volume fraction of the secondary phase GeO_2 is 2.41% (Table 2) it has no significant impact on the overall process of crystallization of the glass. Therefore, the behaviour of the first exothermal peak T_{p1} which belongs to the main $LiGe_2(PO_4)_3$ crystalline phase was analysed. The results of DTA experiment with different glass particle size (Fig. 3) showed that in the range of the smallest granulations the surface mechanism of crystallization is dominant. With increasing particle size the surface mechanism of crystallization is replaced by the volume one, and in the size range > 0.4 mm the volume mechanism of crystallization prevails.

For determination of the kinetic parameters of crystallization the equation for the analysis of non-isothermal crystallization derived by Matusita and Sakka [13] was used:

$$\ln \frac{\beta^n}{T_p^2} = -\frac{m \cdot E_a}{R \cdot T_p} + const. \qquad (1)$$

where R is the gas constant, and E_a is activation energy of crystal growth. The values of the parameters n and m depend on the rate controlling mechanism of the crystallization kinetics. The DTA experiment was performed with the glass powder of the smallest particle sizes (< 0.048 mm) where the surface crystallization dominates and the number of nuclei is constant during DTA run at different heating rates β. In this case $n = m = 1$ and equation (1) becomes the same as the well-known Kissinger equation [14]. Using the DTA data (Table 3), the activation energy of crystal growth of E_a = 462 ±11 kJ/mol was calculated from the slope of the line of the Kissinger plot ln(β/T_p^2) *vs.* 1/T_p, Fig. 5.

The DTA experiments with the powder glass samples revealed that in the particle size range >0.4 mm the volume mechanism of crystallization is dominant for this glass. To determine the temperature range of nucleation and the temperature of maximum nucleation rate the samples with particle sizes 0.50–0.65 mm previously nucleated at selected temperatures T = 500–620 °C for

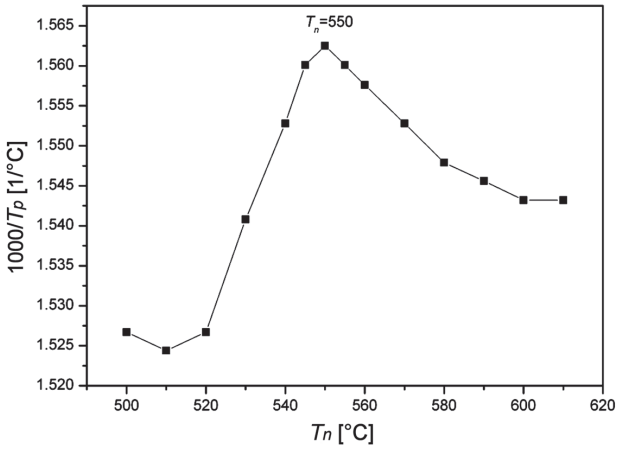

Figure 6. The dependence of T_p^{-1} on T_n for glass sample nucleated for t = 30 min

different times t_n = 15–300 min were heated in DTA apparatus at heating rate β = 10 °C/min. A plot of inverse exothermal peak temperature T_p^{-1} vs. nucleation temperature T_n produces a nucleation rate-like which agree reasonably with the determined temperature range of nucleation and the temperature of maximum nucleation rate [15]. In Fig. 6 the dependence of T_p^{-1} on T_n for the glass sample nucleated for t = 30 min is shown. The nucleation-like curve in the temperature range from 510 to 600 °C shows a maximum at T_n = 550 °C, commonly called the temperature of maximum nucleation, Fig. 6. At this temperature, the nucleation rate $I_{550} = 6.42\times10^{16}$ $m^{-3}s^{-1}$ and crystal growth rate $u_{550} = 1.42\times10^{-11}$ m/s were determined by using the SEM analysis of isothermally heated bulk glass samples.

V. Conclusions

The glass-ceramics was obtained by crystallization of the parent glass composition of $22.5Li_2O{\cdot}10Al_2O_3{\cdot}30GeO_2{\cdot}37.5P_2O_5$ (mol%) prepared by standard melt-quenching technique. The NASICON-type $LiGe_2(PO_4)_3$ crystals precipitated as a major phase in the glass matrix. The small volume fraction of secondary GeO_2 phase was detected in the samples. SEM analyses showed that the crystallization process occurred with high homogeneous nucleation rate and spherical crystal growth morphology. The nanostructured glass-ceramics samples were obtained. The temperature range of nucleation T = 510–600 °C and the temperature of maximum nucleation T_n = 550 °C were determined for the parent glass. It was shown that the mechanism of crystallization depends on glass particle size and the dominant volume that was determined for the glass with particle sizes >0.4 mm. The value of activation energy for crystal growth E_a = 462±11 kJ/mol was determined by using the Kissinger relation.

Acknowledgments: The authors are grateful to the Ministry of Education, Science and Technological Development of the Republic of Serbia for financial support (Projects 34001 and 172004).

References

1. N. Anantharamulu, K.K. Rao, G. Rambabu, B.V. Kumar, V. Radha, M. Vithal, "A wide-ranging review on Nasicon type materials", *J. Mater. Sci*., **46** (2011) 2821–2837.
2. A.M. Cruz, E.B. Ferreira, A.C.M. Rodrigues, "Controlled crystallization and ionic conductivity of nanostructured $LiAlGePO_4$ glass-ceramic", *J. Non-Cryst. Solids*, **355** (2009) 2295–2301.
3. P. Knauth, "Inorganic solid Li ion conductors: An overview", *Solid State Ionics*, **180** (2009) 911–916.
4. J.W. Fergus, "Ceramics and polymeric solid electrolytes for lithium-ion batteries", *J. Power Sources*, **195** (2010) 4554–4569.
5. H. Aono, E. Sugimoto, Y. Sadaoka, N. Imanaka, G. Adachi, "Ionic conductivity of solid electrolytes based on lithium titanium phosphate", *J. Electrochem. Soc.*, **137** [4] (1990) 1023–1027.
6. S. Matijašević, "Crystallization behaviour of multicomponent germanate glasses", *Doctoral dissertation*, TMF, University of Belgrade, 2012.
7. H.M. Rietveld, "A profile refinement method for nuclear and magnetic structures", *J. Appl. Cryst.*, **2** (1969) 65–71.
8. J. Rodriguez-Carvajal, "User's guide to program FULLPROF", 2004-LLB-JRC (Laboratorie León Brillouin, CEA-CNRS, Centre d'Etudes de Saclay, Gif sur Yvette, France), 1995.
9. $LiGe_2(PO_4)_3$-JCPDS Powder Diffraction File, Card No. 80-1922, Joint Committee on Powder Diffraction Standards (JCPDS), Swarthmore, PA.
10. GeO_2-JCPDS Powder Diffraction File, Card No. 83-0543, Joint Committee on Powder Diffraction Standards (JCPDS), Swarthmore, PA.
11. R.K. Brow, "Review: The structure of simple phosphate glasses", *J. Non-Cryst. Solids*, **263-264** (2000) 1–28.
12. C.S. Ray, Q. Yang, W. Haung, D.E. Day, "Surface and internal crystallization in glasses as determined by differential thermal analysis", *J. Am. Ceram. Soc.*, **79** (1996) 3155–3160.
13. K. Matusita, S. Sakka, "Kinetic study on crystallization of glass by differential thermal analysis:criterion on application of Kissinger plot", *J. Non-Cryst. Solids*, **38-39** (1980) 741–746.
14. H.E. Kissinger, "Reaction in differential thermal analysis", *Anal. Chem.*, **29** (1959) 1702–1706.
15. A. Marotta, A. Buri, F. Branda, "Nucleation in glass and differential thermal analysis", *J. Mater. Sci.*, **16** (1981) 341–344.